



biblio.ugent.be

The UGent Institutional Repository is the electronic archiving and dissemination platform for all UGent research publications. Ghent University has implemented a mandate stipulating that all academic publications of UGent researchers should be deposited and archived in this repository. Except for items where current copyright restrictions apply, these papers are available in Open Access.

This item is the archived peer-reviewed author-version of: Technical implementations of light sheet microscopy

Authors: Zagato E., Brans T., De Smedt S.C., Remaut K., Neyts K., Braeckmans K.

In: Microscopy Research and Technique, 81(9): 941-958

To refer to or to cite this work, please use the citation to the published version:

Van Zagato E., Brans T., De Smedt S.C., Remaut K., Neyts K., Braeckmans K. (2018) Technical implementations of light sheet microscopy

Microscopy Research and Technique, 81(9): 941-958

DOI: 10.1002/jemt.22981

TITLE PAGE

Technical implementations of light sheet microscopy

Authors, Affiliation and mail addresses

Zagato Elisa, Laboratory of General Biochemistry and Physical Pharmacy, Ghent University, Belgium;
Center for Nano- and Biophotonics, Ghent University, Belgium; zagato.elisa@gmail.com

Brans Toon, Laboratory of General Biochemistry and Physical Pharmacy, Ghent University, Belgium;
Center for Nano- and Biophotonics, Ghent University, Belgium; toon.brans@ugent.be

De Smedt Stefaan, Laboratory of General Biochemistry and Physical Pharmacy, Ghent University,
Belgium; stefaan.desmedt@ugent.be

Remaut Katrien, Laboratory of General Biochemistry and Physical Pharmacy, Ghent University, Belgium;
katrien.remaut@ugent.be

Neyts Kristiaan, Center for Nano- and Biophotonics, Ghent University, Belgium; Liquid Crystals and
Photonics Group, Ghent University, Belgium; kneys@elis.ugent.be

Corresponding author:

Braeckmans Kevin, Laboratory of General Biochemistry and Physical Pharmacy, Ghent University,
Belgium; Center for Nano- and Biophotonics, Ghent University, Belgium; kevin.braeckmans@ugent.be

Keywords

Light sheet microscopy, SPIM.

Research Highlights

We present an overview of recent technological advances in Light-Sheet Fluorescence Microscopy (LSFM). The focus will be on custom-built set-ups as well as commercially available LSFM microscopes. Special attention goes to designs that allow integration of LSFM on standard microscope bodies.

Abstract

Fluorescence-based microscopy is among the most successful methods in biological studies. It played a critical role in the visualization of subcellular structures and in the analysis of complex cellular processes, and it is nowadays commonly employed in genetic and drug screenings. Among the fluorescence-based microscopy techniques, light sheet fluorescence microscopy (LSFM) has shown a quite interesting set of benefits. The technique combines the speed of epi-fluorescence acquisition with the optical sectioning capability typical of confocal microscopes. Its unique configuration allows the excitation of only a thin plane of the sample, thus fast, high resolution imaging deep inside tissues is nowadays achievable. The low peak intensity with which the sample is illuminated diminishes phototoxic effects and decreases photobleaching of fluorophores, ensuring data collection for days with minimal adverse consequences on the sample. It is no surprise that LSFM applications have raised in just few years and the technique has been applied to study a wide variety of samples, from whole organism, to tissues, to cell clusters and single cells. As a consequence, in recent years numerous set-ups have been developed, each one optimized for the type of sample in use and the requirements of the question at hand. Hereby we aim to review the most advanced LSFM implementations in order to assist new LSFM users in the choice of the LSFM set-up that suits their needs best. We also focus on new commercial microscopes and “do-it-yourself” strategies; likewise we review recent designs that allow a swift integration of LSFM on existing microscopes.

TEXT

Introduction

Nowadays, fluorescence microscopy has become an important tool for biologists to make sense of the biological world. The ability to conjugate fluorophores with almost any existing molecule, or even to induce cells to produce their own fluorescent proteins, has opened up tremendous possibilities to visualize subcellular structures with high resolution and superior contrast. Total internal reflection fluorescence (TIRF), epi-fluorescence, scanning confocal and spinning disk confocal microscopes are among the most common set-ups, available in almost every research facility that works with cells. Each of these microscope techniques have their assets, but also some limitations. Epi-fluorescence microscopes are well-suited for fast acquisition of dynamics processes, but suffer from low axial resolution and their inability to remove out-of-focus fluorescence. Confocal microscopes fare way better in that respect. While inherently slower, their optical sectioning capability allows for a stunning improvement of contrast and axial resolution compared to widefield epi-fluorescence illumination. However, optical sectioning is achieved by rejecting the out-of-focus light through a single pinhole or a pinhole array. As a consequence, the whole sample has to be irradiated by a high intensity excitation laser beam, leading to a sub-optimal usage of the fluorophore photon budget and increased photo-damage to the sample under observation. TIRF microscopy is gentler towards the specimen, since it stimulates fluorescence only in one plane in the sample of 100-200 nm thickness. Sadly, it's the plane just on top of the coverslip, so that no information whatsoever can be obtained from deeper regions inside the specimen. In recent times a very interesting technique, that combines several of the advantages of the aforementioned systems, has become available to the research community. This technique is called Light Sheet Fluorescence Microscopy (LSFM), also known as single/selective plane illumination microscopy (SPIM), and enables high resolution, multidimensional (3D+t) imaging of extended 3D samples for extended periods of time with limited phototoxic effects. As explained further in this review, LSFM set-ups vary much from developer to developer due to the specific needs of the sample under observation and the scientific questions being asked. However, with few notable exceptions, they all have in common that they require an objective lens that illuminates a plane in the sample that coincides with the focal plane of the objective lens used for detection, as illustrated in Fig. 1.

The sample is usually mounted into a special sample holder compatible with an orthogonal illumination and imaging configuration. Since only the plane under observation is illuminated, out-of-focus excitation is kept at a minimum and high contrast images can be acquired at fast rates essentially limited by the speed of the camera. The lower light dose the sample receives, especially when recording 3D images, makes LSFM a gentler and less invasive modality to image photosensitive samples which are prone to photobleaching or phototoxicity. Moreover, thanks to its simple set-up and widefield-like detection, the technique lends itself to be combined with superresolution microscopy (STED/RESOLFT (Friedrich, Gan, Ermolayev and Harms, 2011; Gohn-Kreuz and Rohrbach, 2016; Hoyer et al., 2016; Scheul, Wang and Vial, 2014), PALM/STORM/IML (Cella Zanacchi, Lavagnino, Faretta, Furia and Diaspro, 2013; Cella Zanacchi et al., 2011; Greiss, Deligiannaki, Jung, Gaul and Braun, 2016; Hu, Zimmerley, Li, Watters and Cang, 2014; Palayret et al., 2015), SIM (Keller et al., 2010; Planchon et al., 2011; Zhao et al., 2014)), techniques based on fluorescence fluctuation (FFS, FCS (Chen et al., 2016; Krieger, Singh, Garbe, Wohland and Langowski, 2014)) as well as other advanced microscopy and spectroscopy techniques (Raman (Rocha-Mendoza et al., 2015), Tomography (Bassi, Schmid and Huysken, 2015)).

In the last decades, LSFM has been repeatedly put to the test. Although initially developed to study embryonic development (Huisken and Stainier, 2007; 2009; Huisken, Swoger, Del Bene, Wittbrodt and Stelzer, 2004; Lemon and Keller, 2015; Udan, Piazza, Hsu, Hadjantonakis and Dickinson, 2014; Weber, Mickoleit and Huisken, 2014), it has soon found application in the most disparate fields, from developmental biology (Weber and Huisken, 2015) to marine biology (Capoulade, Reynaud and Wachsmuth, 2013); from single cells to spheroids (Smyrek and Stelzer, 2017), up till whole organs like heart and vasculature (Fei et al., 2016; Trivedi et al., 2015), the guts (Taormina et al., 2012), the brain and nervous systems (Gualda, Simao, Pinto, Alves and Brito, 2014; Keller and Ahrens, 2015; Keller, Ahrens and Freeman, 2015; Silvestri, Bria, Sacconi, Iannello and Pavone, 2012; Wolf et al., 2015), the lymph nodes (Abe et al., 2016), pancreatic islets (Lavagnino et al., 2016a), and even the development of plants (Novak, Kucharova, Ovecká, Komis and Samaj, 2015; Ovecká et al., 2015). However, despite its demonstrated value for a wide range of applications, a widespread diffusion of LSFM is still lacking. Indeed, while first LSFM instruments are gradually becoming commercialized, in most cases LSFM set-ups are home-built according to a variety of designs depending on the application at hand. Therefore, in this review a succinct overview is provided of the most advanced LSFM modalities with their advantages and disadvantages, aimed at guiding the interested researcher to choose the LSFM set-up that best suits a particular application. In the second part of this review, the focus will be on the commercially available LSFM microscopes and on recent designs that allow swift integration of LSFM on existing microscopes.

Principle and rationale of light sheet fluorescence microscopy

The idea behind LSFM is to avoid unnecessary exposure of the sample to potentially toxic laser light by illuminating only a single, thin plane in the sample that coincides with the focal plane of the detection lens (see Fig. 1). In its traditional configuration (Huisken et al., 2004; Voie, Burns and Spelman, 1993), an orthogonal light sheet microscope is composed of three distinct components: the excitation arm, the sample holder and the detection arm. The main role of the excitation arm is to shape the laser beam into a light sheet whose thickness essentially determines the optical sectioning capability of the technique. The detection arm determines the lateral and to a large extent the axial resolution as well as the temporal resolution, although in practice the latter is also influenced by the signal to noise ratio, which depends on the intensity of the excitation beam and labeling quality. The combination of the point spread function (PSF) of the illumination and the detection systems, shown in Fig. 2A, leads to an increased axial resolution compared to widefield microscopes. Given the peculiar configuration of LSFM microscopes, special care must be taken to design a sample holder that places the sample at the required distance between the orthogonal objective lenses, while ensuring sample viability and keeping it stable in position. In the following section the major components of LSFM will be discussed in more detail.

Excitation

The excitation light sheet, as shown in Fig. 2C and 2D, may be static or dynamic. A static light sheet is generated by placing a cylindrical lens in the illumination optical path. The set-up is simple and the entire illumination power is spread over the entire field of view, allowing for fast image acquisition. On the contrary, dynamic light sheets, also called digital scanned light sheet microscopy (DSLM), make use of galvanometric mirrors to scan the orthogonal plane with a spherical Gaussian beam so to create a “plane of light” (Keller, Schmidt, Wittbrodt and Stelzer, 2008). Dynamic light sheets focus their entire illumination power on a single line and scan the focal plane so as to emulate a light sheet. As a consequence, dynamic light sheets are more homogenous than static ones. In addition, because the illumination is incoherent it is less affected by scatter than static light sheets. As a consequence, imaging artifacts due to obstacles and denser regions in the sample are reduced, improving the image quality compared to static light sheets (Pampaloni, Chang and Stelzer).

Important characteristics of the light sheet are its beam waist W_0 , and the distance over which the beam's thickness remains fairly uniform, called depth of field (DoF). Conventional light sheets are created with a Gaussian beam, shown in Fig. 2B, whose DoF is proportional to its beam waist. For example, a Gaussian beam with a 1- μm -thick beam waist has a DoF of nearly 13 μm at 488 nm wavelength. Gaussian beams are primarily determined by the numerical aperture NA of the illumination lens, so that cylindrical lenses with low NA are preferred to obtain a light sheet with a large DoF at the expense of a lower axial resolution (i.e. larger beam waist) and reduced optical sectioning.

Care must be taken when imaging large and dense samples, to avoid excessive striping artefacts. As clearly shown in Figure 3, stripes are common in LSFM images. These are caused by all kinds of obstacles that distort the excitation light beam upon its path through the sample, including opaque regions, scattering structures, and impurities or bubbles in the clearing liquid. Several destriping algorithms have been developed (Chang, Fang, Yan and Liu, 2013; Fehrenbach, Weiss and Lorenzo, 2012; Gadallah, Csillag and Smith, 2000; Liang et al., 2016; Münch, Trtik, Marone and Stampanoni, 2009). Most of them are designed for light sheets coming only from one side and are not suited for more complex noise patterns (Liang et

al., 2016). In any case, strategies that avoid stripes formation are to be preferred whenever it is possible. For example, Huisken and coworkers proved that by quickly tilting or pivoting the beam (Huisken and Stainier, 2007), stripe artifacts and aberrations are reduced and the quality of the image of thick specimens is highly improved.

Detection

On the detection side, the detection path consist of an imaging objective lens, an emission filter, tube lens and camera. The NA of the imaging objective lens must be carefully considered since it determines the lateral and axial resolution of the image, as shown in Fig. 2A. The effective available resolution in the image is also partially influenced by the spatial and temporal resolution of the camera, i.e. its pixel density and frame rate. Typically, EMCCD cameras are chosen for their high level of sensitivity that allow faster acquisition times. However, they generally have rather large pixels and, therefore, less spatial sampling and in some cases a limited field of view; instead, modern scientific CMOS cameras are preferred for their improved signal to noise ratio (SNR) detection properties, faster readout and for their high spatial and temporal resolution. Scientific CMOS cameras also may be operated in two data acquisition modes: global shutter, i.e. all the pixels are simultaneously active, and rolling shutter, i.e. only a few adjacent lines are active (Baumgart and Kubitscheck, 2012). As discussed in section DETECTION PATWAY, a clever use of the rolling shutter mode may be beneficial to enhance contrast and increase the image quality.

Sample holder

A LSF microscope is the instrument of choice for long term 3D imaging of live and fixed systems. Although originally implemented in developmental biology, nowadays LSFM applications range from single molecule studies to three dimensional cultures, from fixed and cleared samples to *in vivo* studies. Such a wide range of applications, combined with LSFM unique configuration which makes its implementation on common microscopes challenging, has given rise to a range of atypical, tailor-made sample holders. Well-designed sample holders should fulfill three main requirements (Guetiérrez-Heredia, Flood and Reynaud, 2012). First of all, mechanical stability during imaging is a key feature. The specimen must be well supported to avoid deformation during rotation or sample movements. Second, it is of the utmost importance to employ sample holders that cause minimal light distortion. For example, the materials employed should have a refractive index as close as possible to the refractive index of the medium in which the sample is embedded. Third, the viability of the specimen is extremely important for long acquisition experiments. Thus the specimen should be well supported and still be able to grow, while at the same time receive the necessary nutrients. Fig. 2E shows the most typical sample holders (Guetiérrez-Heredia et al., 2012; Krieger et al., 2015; Reynaud, Peychl, Huisken and Tomančák, 2015). The most common sample holders position the objective lenses inside a water filled chamber. The sample, typically embryos or cell clusters, is embedded inside a soft gel, usually low-melting agarose or specialized hydrogels, and it is extruded from a capillary inside the chamber. However, care must be taken to monitor the development of the sample, since mechanical forces exerted by the gel are known to be responsible of malformation (Kaufmann, Mickoleit, Weber and Huisken, 2012). Large samples as well as tissues may instead be kept in position by a sterilized hook. Liquid samples like beads in a solvent are best mounted in a transparent, heat sealed plastic bag made from fluorinated poly-ethylene-propylene films (Krieger et al., 2015). Small cell clusters and spheroids may be pumped through a channel and imaged while they are flowing through the light sheet (Meddens et al., 2016; Paie, Bragheri, Bassi and Osellame, 2016). Lastly,

adherent cells are plated onto small cover glass pieces and positioned in the sample chamber at an angle between the coverslip and the illumination objective lens. It is advisable to not choose an angle of 45° between the coverslip and the illumination objective, since at that angle excitation light reflected by the water/glass interface will reach the camera as well and degrade contrast.

Recent technological developments

A LSFM is the ideal technique to follow fast, dynamic processes that happen in a 3D biological environment. To obtain robust, reliable data, it is crucial that LSFM provides a high spatiotemporal resolution, ultralow photobleaching rates and an excellent signal to noise ratio SNR. However, imaging large, living specimens using a basic set-up remains challenging. The light sheet has to travel into an inhomogeneous environment with highly absorptive and scattering properties. Not only stripe artifacts due to small regions of higher refraction index are inevitable, but also the SNR can be substantially reduced by out-of-focus fluorescence excited by excitation light scattered in the sample. As a consequence, as the optical path length increases the image quality decreases. In this section we present recent developments to overcome these issues. The most straightforward solution is to collect images of the sample from multiple angles, by simply rotating the sample or by employing multiple objective lenses, and then fuse the collected images together to form a 3D rendering of the sample. Another viable option would be to use a non-diffracting, propagation invariant beam instead of the more typical Gaussian excitation beams. Thanks to their self-healing properties, they can propagate intact deep into scattering samples and increase temporal and spatial resolution. Two photon excitation is also a viable strategy, since it generates a thinner light sheet, avoids unwanted background excitation and reduces photobleaching. Lastly, a thoughtful modification of the detection pathway may increase contrast and acquisition speed.

Multiview SPIM

Imaging large, living specimens is a tough job due to the highly absorptive and scattering environment in which light has to travel. As Fig. 4A clearly shows, one-sided illumination results in decreasing image quality along the excitation axis due to the deteriorating effect of scattering of the excitation light sheet that results in out-of-focus fluorescence. These problems may be reduced by so-called multiview sample reconstruction. The idea is to collect multiple image stacks at different angles. If necessary, the image stacks are deconvolved and then fused together to reconstruct a 3D image of the sample. Thanks to multiview reconstruction, the uniformity of the image quality is improved in strongly scattering and absorbing samples, while in transparent samples the axial resolution is strongly enhanced, to the point that the resolution becomes isotropic. Fig. 4 shows the most common configurations that allow multiview reconstruction. In the first SPIM set-up, proposed by Huisken et al. (2004), the light sheet is generated inside a buffer-filled chamber. The sample is immersed into the buffer from the top. It can thus be rotated to allow the collection of image stacks from multiple angles on the same sample. Such a system has been used successfully to image fixed *Medaka* and live *Drosophila melanogaster* embryos (Huisken et al., 2004; Swoger, Verveer, Greger, Huisken and Stelzer, 2007). However, multiview reconstruction through sample rotation presents several disadvantages (Krzic, Gunther, Saunders, Streichan and Hufnagel, 2012). First, due to the difficulties in the precise determination of the axis of rotation relative to the specimen, the images are inherently misaligned. The use of computationally intensive and unreliable image registration algorithms may be necessary to align the images. Second, sample rotation is sometimes slower than the

biological dynamics under observation. Lastly, the quality of the image increase with the number of viewing directions. As a consequence, not only the time resolution decreases, but also the sample is exposed to a higher dose of light than in a basic light sheet microscope, increasing photobleaching and phototoxic effects.

The need to collect high SNR images of opaque specimens while retaining its high temporal resolution and low phototoxicity has led to the development of dual excitation LSFM set-ups. The simpler solution is to add a third objective lens so that the sample can be illuminated from two sides (Keller et al., 2008), as it was done in mSPIM (Huisken and Stainier, 2007), shown in Fig. 4C. In mSPIM the light sheet is sequentially directed onto the sample from two opposing directions. For faster image acquisition, a fourth lens, used for detection, may be beneficial. This set-up is shown in Fig. 4D and is called MuVi-SPIM (Krzic et al., 2012). The system consists of four objective lenses, two for illumination and two for detection, placed into a fixed geometrical arrangement for multiview data fusion in real time. Both detection objective lenses are focused onto a common focal plane, illuminated alternately by the two dynamic light sheets. Both detection arms are used simultaneously to increase light efficiency. The illumination arms work in an alternated fashion to avoid image blur due to increased scattering coming from two light sheets at the same time. The specimen is positioned in the sample chamber that is moved through the light sheet by a fast piezo stage. While there is no need to rotate the sample, to better resolve small structures, it is recommended to rotate the sample over 90° at least once. Similar to MuVi-SPIM is SiMView (Ahrens, Orger, Robson, Li and Keller, 2013; Tomer, Khairy, Amat and Keller, 2012), a four-armed light sheet microscope which features single photon and multiphoton excitation. Their automated software modules ensure perfect alignment of the light sheets and the detection optics, to increase spatiotemporal resolution. Both mSPIM, MuVi SPIM and SiMView have been used to successfully image, faster than in conventional SPIM, *Drosophila Melanogaster* embryos (de Medeiros et al., 2015; Krzic et al., 2012; Tomer et al., 2012) and live *Zebrafish* (Ahrens et al., 2013; Huisken and Stainier, 2007). Last but not least, Wu et al. developed a new LSFM with high isotropic spatial resolution in all dimensions (Wu et al., 2013). The set-up is built on a dual inverted SPIM (iSPIM) microscope, shown in Fig. 4E. Two objective lenses are placed orthogonally to each other and are both used alternately for illumination and detection. The combination of the two perpendicular views with their self-developed “joint deconvolution method” resulted in an impressive isotropic resolution of 330 nm (NA 0.8), quadrupling the axial resolution as well as improving upon the lateral resolution. The technique retains the LSFM advantages previously described in this section, but has a faster acquisition speed and presents isotropic resolution.

Engineered Light Sheets

A key property of LSFM is its excellent optical sectioning ability. Indeed the light sheet thickness, in combination with the NA of the detection lens, determines the axial resolution in the image and its contrast. For conventional light sheets created with Gaussian beams, beam thickness and depth of field are proportional to each other, as previously described. Hence a Gaussian light sheet uniform for several tens of micrometers requires a relatively thick beam waist, which in some application would compromise the axial resolution, expose the sample to unnecessary light irradiation and preclude the application of the technique to sub-cellular studies. Moreover, beams traveling for hundreds of micrometers inside an inhomogeneous environment, such as biological tissues, are usually deformed by obstacles in the light path, with consequences on the image quality. As a consequence, a Gaussian beam is not necessarily the best choice for intracellular studies that require high contrast and high axial resolution over an extended

field of view (*FoV*) spanning tens of microns. The ideal light sheet for that kind of application should preferably be consistently thin over the entire specimen. In addition it would be beneficial if the beam has the ability to re-form after being partially obstructed (that is, it has 'self-healing' properties) to overcome aberrations induced by imaging deep into tissues. As such it is of interest to look into non-diffracting, propagation-invariant beams. Various reports have emerged over the past few years evaluating Bessel beams (Andilla et al., 2017; Fahrbach, Gurchenkov, Alessandri, Nassoy and Rohrbach, 2013b; Fahrbach and Rohrbach, 2010; 2012; Gao, Shao, Chen and Betzig, 2014; Gohn-Kreuz and Rohrbach, 2016; Zhang, Phipps, Goodwin and Werner, 2016; Zhao et al., 2014; Zhao et al., 2016) and Airy beams (Vettenburg et al., 2014) for LSFM, shown in Fig. 5. Bessel beams are the most used as they are fairly easy to implement. Bessel beams are generated by focusing a Gaussian beam on an axicon lens (Gao et al., 2014), by using a spatial light modulator (Chen et al., 2014; Fahrbach and Rohrbach, 2010) or by projecting an annular illumination pattern at the rear pupil of the excitation objective lens (Planchon et al., 2011). Although Bessel beams have the ability to produce light sheets with a *FoV* 3-5 times longer than a Gaussian *FoV* (Planchon et al., 2011), they suffer from a suboptimal SNR due to the presence of quite pronounced side lobes in the diffraction pattern. While the majority of the beam energy is concentrated in the central peak, a substantial amount of energy still resides in the transversal outer ring structure of Bessel beams. In single photon excitation this means that substantial fluorescence is coming from above and below the central light sheet.

Thus, when using Bessel beams in LSFM, strategies to remove or suppress side-lobes fluorescent emission are required. The most common strategies make use of confocal scanning detection (Fahrbach and Rohrbach, 2012), structured illumination (SI) (Chen et al., 2014; Keller et al., 2010; Planchon et al., 2011; Zhao et al., 2014) or two-photon excitation 2PE (Collier, Awasthi, Lieu and Chan, 2015; Fahrbach, Gurchenkov, Alessandri, Nassoy and Rohrbach, 2013a; Olarte et al., 2012; Planchon et al., 2011). Briefly, in confocal scanning detection mode the image is acquired line-wise. A single pixel-line records a one-dimensional image at the position of the beam, so that only the part illuminated by the Bessel beam central lobe is recorded. As a consequence, the probability of recording photons emitted in the region illuminated by the side lobes is decreased, providing enhanced contrast and higher axial resolution. High contrast images are thus directly recorded by the camera with no need of image post-processing, as it is the case when using SI. In that case a resolvable multi-harmonic excitation pattern is generated. N such images are then acquired, with the pattern phase in each image shifted by $2\pi/N$. The combined final image retain the strongly modulated signal near the focal plane, while the weak contributions from the out of focus regions are discarded. Both the confocal detection and the SI approaches increase the axial resolution and SNR but at the expense of substantial fluorescent signal rejection (up to 90%) (Vettenburg et al., 2014) and temporal resolution. The excessive sample irradiation still excites out-of-focus fluorophores, thus spoiling the overall photon budget unnecessarily. Instead, 2PE excitation with Bessel beams offers the possibility to suppress side lobes and effectively provides a thin sheet with no need for out-of-focus light rejection. The disadvantage, however, is that the set-up is more complex. Moreover to image spectrally different fluorophores at the same time it may be necessary to build a second illumination arm to avoid losing time retuning and realigning the set-up every time a different wavelength is used (Planchon et al., 2011).

The best Bessel-based set-up in terms of spatiotemporal resolution and reduced phototoxicity has been developed by Chen et al. (2014). They used non-diffracting Bessel beams to create a 2D optical lattice which propagates in the sample while keeping its cross-sectional profile unchanged, as seen in Fig. 5. To

create the lattice, the laser light is diffracted by a spatial light modulator conjugated with the sample plane, filtered by an annular mask and then focused on the sample by the objective lens. The microscope can be used as a traditional dithered, digitally scanned light sheet microscope or in combination with structured illumination, depending if temporal or axial resolution has priority. Indeed, imaging in dithered mode is 7.5 times faster than in combination with SI, at a comparable SNR, while the axial resolution is only 1.5 times poorer. Although a bigger region of the sample is illuminated compared to traditional Bessel beams, the peak intensity is lower. The lower peak intensity seems linked to the lower phototoxic effects noticed by Chen et al., which managed to collect 1 and 2 order of magnitude more images before noticing phototoxic effects compared to Bessel beams and confocal microscopy, respectively. Reportedly, a major advantage is the acquisition speed, that ranges between 200 to 1000 planes/s in dithered mode, which is one order of magnitude more than with classic Bessel beams. The technique is undoubtedly very effective, but the set-up is quite complex and the use of a SLM reduces the temporal resolution when multicolor imaging is required since the SLM must be rapidly switched and synchronized with every color change (Zhao et al., 2016). The solution proposed by Zhao et al. (2016) is to use a combination of “non-electronic” optical components to create ultrathin Bessel sheets of the same thickness regardless of the input laser light, as long as it is in the visible range. The excitation light passes first through a slit to give it a line-shape, then through an annulus imaged to the back focal plane of the illumination objective. Two combinations of line-thickness and annulus are designed and tested, one optimized to maximize detection efficiency and minimize photobleaching, the other optimized for high resolution.

Another type of self-healing, propagation invariant beam is the Airy beam, shown in Fig. 5. Despite its broad transversal structure, the Airy beam provides high contrast thanks to its asymmetric excitation pattern (Vettenburg et al., 2014). A simple deconvolution is able to account for both its broad main lobe and its curved profile, yielding high contrast and resolution for its entire *FoV*, that is 10 times and 4 times longer than with Gaussian and Bessel beams respectively. Airy beams are usually generated using a SLM, but an approximated Airy beam can also be generated by correctly tilting cylindrical lenses (Yang et al., 2014).

Despite these many technological improvements, the quest for ever bigger *FoV* with maximal optical sectioning goes on. Recently Gao and coworkers (Fu, Martin, Matus and Gao, 2016; Gao, 2015) proposed a new technique that gives the possibility to choose the best light sheet required for the experiment while extending its *FoV*. The principle is fairly simple, as shown in Fig. 6.

Instead of generating a large and uniform light sheet, their microscope generates a thinner and shorter light sheet that is moved in multiple positions within the image plane. Only the signal from the center of the light sheet is recorded for every position and large *FoV* image is finally obtained by stitching all those images together.

The microscope is made to be quite versatile: the light sheet is generated by two SLM, one used for the amplitude of the signal, the other to modulate the phase of the beam, that can thus quickly be defocused to move it within the image plane. As a consequence, the microscope can adapt more easily to the type of sample and to the light sheet thickness and *FoV* required since every small change can be implemented in one millisecond. The imaging speed is certainly reduced compared to other LSFM techniques like lattice light sheet or airy beam-based microscopy, but with a smart use of modern days CMOS cameras the “temporal loss” may be quite acceptable for many applications.

A similar approach has been chosen by Zong and coworker (Zong et al., 2014; Zong et al., 2015) when they developed their two-photon three-axis digitally scanned light sheet microscope (2P3A-DSLM). They use a tunable acoustic gradient (TAG) index device, shown in Fig. 6B, to quickly scan the focal spot along the illumination axis and two galvanometric mirrors to scan the focal spot on the focal plane of the detection lens and perpendicularly to that plane. The process is so fast that the temporal resolution is only limited by the detection camera and it can provide sheets with submicrometer thickness and a *FoV* ranging anywhere in between $10 \times 10 \mu\text{m}^2$ and $170 \times 170 \mu\text{m}^2$. Table 1 presents a summary of light sheet properties discussed in this section.

Deep into tissues: 2PE microscopy

Apart from particular beam profiles, 2PE LSM has particular benefits for imaging deep inside thick tissues and organisms. NIR light interacts less with biological tissues compared to visible light. Therefore, the 2PE light sheet can penetrate at least two times deeper in biological tissues compared to traditional 1PE light sheets, suffers less from scattering effects and better preserves its shape deep inside scattering tissues (Truong, Supatto, Koos, Choi and Fraser, 2011). Also, NIR light doesn't excite autofluorescence as much as visible light does. On the other side of the coin, a 2PE setup is more complex than a 1PE setup and requires a powerful and costly femtosecond-pulsed laser. As an example, an excitation power of hundreds of mW is necessary to obtain the same signal with 2PE Bessel beams as registered with 1 mW of a 1PE Gaussian beam (Olarde et al., 2012). At such powers, supra-quadratic absorption processes may induce photodamage of fluorophores and tissues (Ji, Magee and Betzig, 2008).

The advantages of combining 2PE and LSM may depend on the type of beam shape. A 2PE Gaussian beam which penetrates deep into the sample ($>90 \mu\text{m}$) (Truong et al., 2011) has indubitably a better image quality thanks to the higher contrast and the reduced background noise, but it also presents a strongly reduced *FoV* (Olarde et al., 2012). Reportedly, it is well-suited for imaging inside scattering samples with high resolution and high fluorescent yield (Olarde et al., 2012). As stated in the previous paragraph, Bessel beams likely benefit the most from 2PE. A recent comparative study shows that 2PE Bessel beams outperform Gaussian beams and 1PE Bessel beams in terms of contrast, resolution and penetration depth. They also offer a large *uniform illumination areas* at the expense of a somewhat poorer SNR (Andilla et al., 2017). 2PE Bessel beam LSM seem to be the perfect combination for following mildly fast dynamics deep ($>150 \mu\text{m}$) inside scattering samples for days, since it combines the contrast-enhancing properties of 2PE, the self-healing properties of Bessel beams and the ability of LSM of reducing light-induced toxicity effects.

2PE LSM has been successfully employed to image not only embryos and their organs (Mahou, Vermot, Beaurepaire and Supatto, 2014; Olarte, Andilla, Artigas and Loza-Alvarez, 2015; Olarte et al., 2012; Truong et al., 2011; Zong et al., 2014; Zong et al., 2015) but also subcellular structures and mechanism inside embryos (like pancreatic islets (Zong et al., 2014), time lapse dynamics of mitochondria (Zong et al., 2015)) and deep inside highly scattering environments like mouse brain slices (Lavagnino et al., 2016b) and tumor cell clusters (Fahrbach et al., 2013a). As said, 2PE multicolor imaging is tricky and may potentially lead to cumulative photodamage. Mahou et al. (2014) use wavelength mixing to achieve fast multicolor 2PE LSM. To achieve wavelength mixing, they spatially and temporally overlapped two different pulse trains (800-nm range and 1100-nm range) for the excitation of blue and red fluorophores, respectively. Their spatiotemporal overlap allows the excitation of a third, green fluorophore. Thus they could image in multicolor the beating heart of a zebrafish embryo labeled with CFP, GFP and DsRed (pericardial,

myocardial and red blood cells, respectively). Unfortunately, photobleaching of the red fluorophore is enhanced by the light required for excitation of the blue fluorophore (800-nm).

The Detection Pathway

In a traditional LSFM setup, the fluorescence detection unit does not differ from the detection unit of a conventional epi-fluorescence microscope. Some recent developments however have shown that a thoughtful modification of the detection path can enhance LSFM performance in terms of contrast, acquisition speed and spectral resolution. As an example, confocal detection is a useful tool to be added to any digitally scanned light sheet microscope which can be achieved with both an EMCCD (Fahrback and Rohrbach, 2012; Silvestri et al., 2012) or a CMOS camera (Baumgart and Kubitscheck, 2012). Silvestri et al. (2012) managed to increase the image contrast obtained using a EMCCD camera in real time with no need of an additional post processing algorithm. A detection de-scanning system is coupled with the digitally scanned light sheet to image the excitation scanning line as a static line in a secondary plane. In this plane a confocal slit is placed, after which a third scanning systems reconstructs the scanned image on the EMCCD camera. On the other hand Baumgart and Kubitscheck (2012) chose to exploit the ability of CMOS cameras to address and read out each pixel independently from each other. Thus the camera itself can be used as a slit detector to enhance contrast and the degree of confocality by simultaneously activating only a portion of consecutive pixel lines. A band of consecutive active pixel rows moves across the sensor in sync with the scanning of the illumination beam. The system doesn't require any additional optical or mechanical components, nor any post processing algorithm. Such a simple and clever concept has been revived by Dean et al. in their axially swept light sheet microscope (ASLM) (Dean, Roudot, Welf, Danuser and Fiolka, 2015) and their diagonally axially swept light sheet microscope (DiASLM) (Dean et al., 2016). In their setup instead of a dynamically scanned light sheet they use a cylindrical lens to create a static light sheet. The microscope scans the light sheet in its direction of propagation synchronously with an array of active pixels on the camera. By activating only the pixels that record the in-focus region of the beam, out-of-focus contributions are discarded over an arbitrarily large FoV . Each plane is acquired in a single exposure with no need of deconvolution. Thanks to this method, the relationship between FoV , W_0 and axial resolution are decoupled, ensuring high illumination uniformity. Thus high contrast, high resolution images can be acquired over a large FoV .

Recording 3-D images with LSFM requires the simultaneous movement in z of the excitation light sheet and imaging objective lens. To avoid having to move the bulky objective lens up and down, which limits the temporal resolution, recently it was suggested to extend the DoF of the detection lens. In that way the excitation light sheet would remain in focus of the objective lens regardless of the light sheet's z -position. It is possible to extend the DoF of the detection optics by making use of wavefront coding (Olarite et al., 2015) or by introducing spherical aberrations (Tomer et al., 2015). The last method is shown in Fig. 7. The only requirement to use wave front coding is to place a suitable phase mask at the exit pupil of the objective lens. All the objects of the sample over the extended DoF are projected to the image plane, thus an appropriate deconvolution is required to reconstruct the final 2D image. A more versatile method to extend the DoF is achieved by placing a block of higher refractive index between the detection lens and the sample. The block introduces uniform spherical aberrations that induce PSF elongation. The microscope is thus able to scan thousands of volumes per second at 1 mm depth while preserving lateral resolution. Both the "wavefront coding" and the "spherical aberration" approaches are perfectly compatible with Airy beam, lattice and Bessel beams, as well as TPE and multidirectional LSFM. However,

they do suffer from low spectral resolution, as many other microscopy techniques do. Hyperspectral approaches have been recently developed to study the interaction of many components in complex biosystems and have been recently applied to LSFM (Jahr, Schmid, Schmied, Fahrbach and Huisken, 2015). The scheme of hyperspectral LSM is presented in Fig. 8 and, as it can be seen, it is applicable only to digitally scanned LSFM. Thanks to a de-scanning mirror and a diffractive unit, for every plane the camera chip records a data cube made of a stack of x, λ data sets. Multi-colors images are then easily obtained by selecting arbitrary, flexible virtual filters. Autofluorescence is thus readily removed or exploited to highlight the structure of the sample. This technique outperforms filter based approaches, not only because of contrast-enhanced detection, but also for its flexibility and its ability to resolve overlapping fluorophores. It's fast since it acquires all the color at once and maintains spatial resolution at a minimal light dose. Such a technique would be beneficial to study the interactions of dozens of components in a sample or to monitor environmental conditions, such as changes in the pH, as long as fluorophores or dyes sensitive to the environmental change are employed.

Widespread diffusion of LSFM

While LSFM is undoubtedly a very valuable addition to the biologist's microscopy toolbox, the advanced configurations discussed above are far from trivial to build and require extensive optics and engineering skills. In order to be truly successful, LSFM should gradually move from the specialized optics laboratory towards user-friendly devices that are available to the broader biological community. Efforts in this direction are ongoing, with construction manuals being made available on the one hand, and first generations of commercial instruments coming to the market on the other hand. In addition, in recent reports concepts are being put forward to implement LSFM on standard microscope bodies.

Commercially available microscopes

In recent years, the LSFM business has expanded enormously. As of January 2015, two such microscopes came to the market. Two years later, already six companies are selling 8 different types of LSFMs, shown in Fig. 9. The first commercialized system is the Lightsheet Z.1, produced by Zeiss. It is based on the set-up introduced by Huisken and Stelzer (Huisken et al., 2004) and it is mainly designed for multiview imaging of large, living specimens, although imaging of cleared specimens is also possible. It is well suited for research in developmental biology and to follow cell dynamics in small model organisms or tissues. The sample, placed vertically into the chamber from above, is illuminated from two sides by a light sheet. The light sheet is rotated to allow fast image recordings from multiple angles, as it is beneficial to increase resolution and information content. The MuVi-SPIM microscope marketed by Luxendo is a valid alternative. Based on the set-up developed by Krzic et al. (Krzic et al., 2012), MuVi-SPIM provides four orthogonal views of the sample with no need for rotation, increasing acquisition speed, long-term stability of the sample and data fusion precision. While MuVi-SPIM is optimized for speed, the InVi-SPIM is more adapted to long-term 3D fluorescent imaging of living specimens. InVi-SPIM is an inverted SPIM microscope with easy access to the sample chamber, that can be customized and autoclaved. It is typically applied on small animal models and mammalian cell culture for 3D reconstruction and tracking of cellular and sub-cellular positions. For large, cleared, fluorescently labeled tissue samples the Ultramicroscope II from LaVisionBioTech, based on the design of Dodt et al. (2007), is a viable alternative. Their software is designed to compensate and correct for different refractive indices induced by the clearing reagents. This bidirectional LSFM generates 6 light sheets, 3 per side from different angles, and shift their focus through

the sample while imaging. As a result, image acquisition is very fast (100 fps at full frame) and stripes and artifacts are reduced. The light sheet width, thickness and *FoV* are user-defined and can cover large areas of the sample, for a high degree of flexibility. The Ultramicroscope II has been successfully used for neurobiology applications and to study neovascularization and lymph nodes, as well as developmental steps in animal models, but at cellular resolution since the minimum light sheet thickness is 4 μm , as declared in the online specifications. At present, the only commercially available microscope that provides an uniform light sheet with sub-micrometer thickness is the Lattice LightSheet microscope from 3i company, based on the set-up of Chen et al. (2014). The creation of a lattice Bessel beam generates a 0.4 μm thin light sheet that extends for 50 μm . The use of a high speed CMOS camera allows collection of images at a 100-500 fps. Samples are simply mounted on a 5 mm round coverslip. It is thus possible to observe with high spatial and temporal resolution cell substructures, cell-cell interaction, single molecule diffusion into spheroids, as well as cell motility in a 3D matrix and embryogenesis.

LSFM can be combined with other microscopy modalities as well. Marianas LightSheet, developed by 3i company, is one of such developed microscopes. It combines a dual inverted SPIM set-up (see Fig. 4E) with the flexibility of an inverted live-cell microscope system. Spinning disk confocal microscopy and TIRF can be added, as well as the lasers and hardware needed for fluorescence life-time imaging microscopy FLIM or for photomanipulation. The diSPIM set up provides high speed imaging (up to 600 fps) at isotropic resolution. It supports conventional sample holders such as coverslips and petri dishes as well as custom-designed chambers, thus it is adapted to image specimens of various sizes, ranging from single cells to whole organisms. Another example of a LSFM designed to be compatible with other microscopy modalities is the TCS SP8 Digital Light Sheet microscope from Leica. Thanks to the addition of the TwinFlect mirror device, they turned their confocal platform into a Reflected Digital Light Sheet microscope. In a reflected light sheet microscope a 45° (micro)mirror is placed close to the sample and it is used to reflect the light sheet perpendicular to the detection lens. In the approach chosen by Leica, they make use of two opposing 45° mirrors that are attached to the condenser lens of the diascope illumination arm. By reflecting and rapidly scanning the laser light coming from the diascope arm, a light sheet is formed in the sample and imaging is performed through the microscope's objective lens. The same microscope can be combined with stimulated emission depletion STED and coherent anti-stokes raman spectroscopy CARS microscopy, but it is also suitable for FLIM measurements and photoactivated localization microscopy PALM. The sample is mounted in a standard glass bottom dish and embedded in agarose gel. It is mostly used to observe embryogenesis and developmental processes of embryos at a maximum speed of 60 fps, but it is not readily suited for imaging adherent cell cultures. Finally, the Alpha³ microscope from PhaseView is a modular light sheet microscope designed to be added to existing microscopes. The scanning speed is only limited by the camera rate, thus it can reach 100 fps at full frame with their CMOS camera. The sample is left stationary. It can perform high-speed volumetric imaging of weak fluorescent specimens as well as live imaging of 3D cell cultures.

Do It Yourself LSFM

Apart from buying a ready-made microscope, it is also possible to build a basic LSFM according to detailed instructions. The integrate OpenSPIM hard- and software platform is an open access initiative for building and adapting SPIM technologies. The idea is to make SPIM technology available to the broad scientific community, also to those without an optics background. Thus, a wiki site has been established (<http://openspim.org>) which contains a list of commercially available parts needed for the set up as well

as a few CAD drawing for custom-made parts. Instructions are explained with pictures that show the building procedures step by step and an OpenSPIM/Fiji software package is available with tutorials on how to use the program and to modify the source code. Three basic configurations are described: single sided illumination/single sided detection, double sided illumination/single sided detection and a double sided illumination/double sided detection. The simplest set up fits on an optical breadboard of 30 x 45 cm and uses one laser. It is developed mainly for developmental studies and embryogenesis. The sample is embedded into agarose gel and extruded from a capillary fixed to a 4D positioning systems that can move the sample in an acrylic water-filled chamber. It is of note that from time to time courses are organized by EMBO to learn how to build the OpenSPIM set up. Also of note, a light sheet microscope made of Lego blocks (Legolish.org) has been recently presented at the Youth Mobile Festival in Barcelona.

Alternatively, it is possible to purchase an inverted SPIM set up from ASI and assemble its parts. The company provides all the necessary hardware except for the objective lenses, lasers and cameras. Videos are available with instructions on how to build the set up and align the microscope.

LSFM on traditional epi-fluorescent microscopes

The typical design of LSFM with two (or more) perpendicular objective lenses makes that it is not readily compatible with existing microscope bodies, thus hindering its widespread use in the biological sciences. This is why some laboratories have tried to develop solutions to implement LSFM on traditional epi-fluorescence microscope bodies that only make use of a single objective lens.

In 2013, our group proposed microfabricated sample holders that would enable high-resolution light sheet imaging on a traditional epi-fluorescence microscope (Deschout et al., 2014). The sample holder is a disposable microfluidic chip made of a planar waveguide on a silicium substrate, shown in Fig. 10A. By butt coupling of a single mode optical fiber to the planar waveguide, a 9- μm -thick light sheet illumination could be achieved in the center of the microfluidic channel. The design has proven valuable for single particle tracking in biological fluid and has shown its potential as a diagnostic tool. However, since the light sheet is fixed in the center of the channel, it has limited use for imaging biological samples. A device that is better suited for imaging multi-cellular structures in vitro up until embryos was developed by Guan et al. (2016). Their plane illumination plugin (PIP) device, shown in Fig. 10B, can be mounted directly on the stage of any epi-fluorescence microscope. It consists of a short sliding rail, on which the optical components and a compact laser diode are mounted, and a small chamber in which the sample, placed into a FEP tube, is kept and aligned to the light sheet. The light sheet thickness and *FoV* can be tuned and can range between 5.5 to 10 μm for the beam waist thickness and between hundreds of micron to mm for the *FoV*. Dual illumination is also an option. Key features of this simple, compact add-on are definitely its easy implementation and low cost (< 500 USD) although it is not suitable for experiments that require high axial resolution.

Another solution that allows light sheet imaging on epi-fluorescent microscopes was presented by Paie et al. (2016) who developed an integrated optofluidic device for high throughput analysis of 3D spheroids on chip. Their optofluidic device, schematically depicted in Fig. 10C, consist of a microfluidic channel through which the sample flows at constant speed. An embedded cylindrical lens focuses the laser light, coming from an optical fiber, in the channel and images are collected while the sample flows through the 5.5- μm -thick light sheet. The continuous flow allows imaging of 300- μm spheroids in less than 2 second per sample.

To enable high resolution LSFM on epi-fluorescent microscope, a simple and interesting concept, depicted in Fig. 10D and 10E, is at the base of the so-called Reflected Light Sheet Microscopy, already described above. One possible configuration consists of delivering the light sheet from the opposite direction of the detection lens and making use of a reflective surface close to the sample so as to reflect the light sheet horizontally into the sample. The solution put forward by Gebhardt and colleagues (Gebhardt et al., 2013) used a tipless AFM cantilever for horizontal reflection of the light sheet beam in adherent cell cultures. They replaced the condenser of the microscope with a vertically mounted high NA objective lens which focused an elliptical Gaussian beam onto the cantilever. The reflected beam generates a submicrometer light sheet, suitable to illuminate single cells as close as 2 μm from the coverslip. Vertical scanning of the sample is achieved by mounting the sample on a x-y-z piezo stage. While a technological feat, this approach requires addition of specially manufactured AFM cantilever holder and separate optics to provide light sheet illumination incident onto the AFM cantilever, all mounted to a fluorescence microscope, which adds another layer of complexity. Similar to this is the design proposed by Greiss and coworkers, who attached a commercially available micropism on a coverslip (Greiss et al., 2016).

A more practical approach would be to provide the light sheet in the sample through the same objective lens that is used for imaging on a fluorescence microscope. Several groups, including ours, developed in parallel microfluidic sample holders with integrated reflective micromirrors which allow horizontal reflection of the excitation light sheet after it passes through the microscope's objective lens (Galland et al., 2015), as shown in Fig. 10E. The sample holder is placed on a normal epi-fluorescence microscope and a beam-shaping unit is used to provide a sheet of light that emerges from the microscope's standard objective lens. Such a design is compatible with high NA objective lenses and only requires appropriate beam shaping, which can be done before the laser beam is sent into the microscope body. The main differences between the reported devices are to be found in the fabrication process. Galland and coworker's sample holders are made of a UV-curable polymer, index matched with the cell medium, and are obtained through replication from a silicon wafer with tilted microchannel walls prepared by anisotropic wet etching and dry etching. Our group tested an alternative process to fabricate a tilted micromirror, based on polishing of a polyimide wafer at a 45° angle. The sample holders, made by gluing the polymer based micromirrors, are then successfully replicated to decrease the fabrication costs per sample holder, with no evident loss in optical quality (Zagato et al., 2017). Meddens et al. (2016) chose to house an etched silicon wafer into five layers of PMMA with channels, as seen in Fig. 11.

Future Outlook and Conclusions

Nearly two decades after the first modern LSFM microscope was developed, LSFM has become a user-friendly, sample-centered microscopy technique that is already fairly well optimized. The wide variety of set-ups developed in recent years have been designed in response to specific sample needs and the particular scientific questions at hand. Small and fairly transparent model organisms, such as *Drosophila Melanogaster* or *C. Elegans*, are now the predominant subject of LSFM research, but it won't be long before larger and more complex organisms are aimed for. Noteworthy is the swept confocally aligned planar excitation microscope (SCAPE), a single-objective LSFM used to image the intact brain of awake behaving mice, and freely moving *Drosophila* larvae (Bouchard et al., 2015).

Integration of LSFM into high-throughput formats is another area of future developments. For instance, drug or genetic screening, as well as the screening for rare events, could be made possible by the combination of flow-through schemes with automated LSFM imaging. Examples are the development of an open-source platform for high-throughput imaging oriented at drug screening (Gualda et al., 2015) or

the integrated optofluidic device for high throughput 3D reconstruction and analysis of spheroids (Paie et al., 2016). Also, the combination of LSFM with flow cytometry provides the possibility of imaging cells in high-throughput (Regmi, Mohan and Mondal, 2013).

The particular arrangement of objective lenses in LSFM requires specialized sample holders, which may pose technical limits to the sample types that can be studied with a particular LSFM configuration. 3D printing may prove useful in the future to more easily develop specific sample holders for particular samples at an acceptable cost. Jeandupeux, Lobjois and Ducommun (2015) are taking advantage of the technique by developing a casting kit for the preparation of a hydrogel multisample holder, fully customizable and adaptable to any shape of the sample. 3D micromachining and printing is expected to soon lead to the development of compact LSFM modules and sample holders that should allow a more widespread diffusion of LSFM among the scientific community. Paie's optofluidic device for imaging of spheroids, fabricated by femtosecond laser micromachining, is another example (Paie et al., 2016).

Some of the compact devices developed to bring light sheet microscopy on traditional microscopes may benefit from the work of Ploschner et al. (2015). They used a spatial light modulator to pre-shape the laser signal in order to obtain a Gaussian or a Bessel light sheet at the distal end of the multi-mode fiber. In order to scan the sample, a series of holographic masks were designed, each of them producing a light sheet in a different plane. Their method produces a 1.2 μm thick light sheet at 50 μm from the fiber facet. Such a method may one day allow *in vivo* endoscopic imaging deep inside biological tissue, but already at present it could prove useful for on-chip light sheet microscopy.

Lastly, the LSFM technique has great combinatory potential. Optical projection tomography, for example, has been used to generate a transmission contrast image that can provide structural context in large organisms (Bassi et al., 2015; Mayer et al., 2014), while magnetic resonance imaging MRI has been used to visualize a whole mouse brain while neural stem cell innervation was simultaneously imaged with LSFM. (Doerr et al., 2017).

Over time, LSFM has steadily matured and is ready to be applied to the biological questions of this era that more and more require complex cell cultures, tissues and organisms instead of mono-cell cultures. The wide range of set-ups available provide several possibilities for imaging such complex samples with high spatio-temporal resolution. At the same time efforts have been made to provide the scientific communities with a variety of commercialized set-ups, as well as recent designs that allow swift implementation of LSFM on existing microscopes. Certainly, as LSFM will diffuse among research laboratories and research facilities alike, new biological findings are expected to come out thanks to the particular advantages of LSFM that are not offered by any other microscopy modality.

Acknowledgements

E. Zagato would like to acknowledge the financial support of the Agency for Innovation by Science and Technology in Belgium. Financial support by the Ghent University Special Research Fund and the Fund for Scientific Research Flanders (FWO, Belgium) is acknowledged with gratitude. The authors declare having no competing financial interests.

References

- Abe J, Ozga AJ, Swoger J, Sharpe J, Ripoll J, Stein JV. 2016. Light sheet fluorescence microscopy for in situ cell interaction analysis in mouse lymph nodes. *J Immunol Methods* 431: 1-10.
- Ahrens MB, Orger MB, Robson DN, Li JM, Keller PJ. 2013. Whole-brain functional imaging at cellular resolution using light-sheet microscopy. *Nat Methods* 10(5): 413-20.
- Andilla J, Jorand R, Olarte OE, Dufour AC, Cazales M, Montagner YL, Ceolato R, Riviere N, Olivo-Marin JC, Loza-Alvarez P, Lorenzo C. 2017. Imaging tissue-mimic with light sheet microscopy: A comparative guideline. *Sci Rep* 7: 44939.
- Bassi A, Schmid B, Huisken J. 2015. Optical tomography complements light sheet microscopy for in toto imaging of zebrafish development. *Development* 142(5): 1016-20.
- Baumgart E, Kubitschek U. 2012. Scanned light sheet microscopy with confocal slit detection. *Opt Express* 20(19): 21805-14.
- Bouchard MB, Voleti V, Mendes CS, Lacefield C, Grueber WB, Mann RS, Bruno RM, Hillman EM. 2015. Swept confocally-aligned planar excitation (SCAPE) microscopy for high speed volumetric imaging of behaving organisms. *Nat Photonics* 9(2): 113-119.
- Capoulade J, Reynaud EG, Wachsmuth M. 2013. Imaging Marine Life with a Thin Light-Sheet. In: *Imaging Marine Life*. Wiley-VCH Verlag GmbH & Co. KGaA. pp 186-209.
- Cella Zanacchi F, Lavagnino Z, Faretta M, Furia L, Diaspro A. 2013. Light-sheet confined super-resolution using two-photon photoactivation. *PLoS One* 8(7): e67667.
- Cella Zanacchi F, Lavagnino Z, Perrone Donnorso M, Del Bue A, Furia L, Faretta M, Diaspro A. 2011. Live-cell 3D super-resolution imaging in thick biological samples. *Nat Methods* 8(12): 1047-9.
- Chang Y, Fang H, Yan L, Liu H. 2013. Robust destriping method with unidirectional total variation and framelet regularization. *Optics express* 21(20): 23307-23323.
- Chen BC, Legant WR, Wang K, Shao L, Milkie DE, Davidson MW, Janetopoulos C, Wu XS, Hammer JA, 3rd, Liu Z, English BP, Mimori-Kiyosue Y, Romero DP, Ritter AT, Lippincott-Schwartz J, Fritz-Laylin L, Mullins RD, Mitchell DM, Bembenek JN, Reymann AC, Bohme R, Grill SW, Wang JT, Seydoux G, Tulu US, Kiehart DP, Betzig E. 2014. Lattice light-sheet microscopy: imaging molecules to embryos at high spatiotemporal resolution. *Science* 346(6208): 1257998.
- Chen X, Zong W, Li R, Zeng Z, Zhao J, Xi P, Chen L, Sun Y. 2016. Two-photon light-sheet nanoscopy by fluorescence fluctuation correlation analysis. *Nanoscale* 8(19): 9982-7.
- Collier BB, Awasthi S, Lieu DK, Chan JW. 2015. Non-linear optical flow cytometry using a scanned, Bessel beam light-sheet. *Sci Rep* 5: 10751.
- de Medeiros G, Norlin N, Gunther S, Albert M, Panavaite L, Fiuza UM, Peri F, Hiiragi T, Krzic U, Hufnagel L. 2015. Confocal multiview light-sheet microscopy. *Nat Commun* 6: 8881.
- Dean KM, Roudot P, Reis CR, Welf ES, Mettlen M, Fiolka R. 2016. Diagonally Scanned Light-Sheet Microscopy for Fast Volumetric Imaging of Adherent Cells. *Biophys J* 110(6): 1456-65.
- Dean KM, Roudot P, Welf ES, Danuser G, Fiolka R. 2015. Deconvolution-free Subcellular Imaging with Axially Swept Light Sheet Microscopy. *Biophys J* 108(12): 2807-15.
- Deschout H, Raemdonck K, Stremersch S, Maoddi P, Mernier G, Renaud P, Jiguet S, Hendrix A, Bracke M, Van den Broecke R, Roding M, Rudemo M, Demeester J, De Smedt SC, Strubbe F, Neyts K, Braeckmans K. 2014. On-chip light sheet illumination enables diagnostic size and concentration measurements of membrane vesicles in biofluids. *Nanoscale* 6(3): 1741-7.
- Dodt HU, Leischner U, Schierloh A, Jahrling N, Mauch CP, Deininger K, Deussing JM, Eder M, Ziegler W, Becker K. 2007. Ultramicroscopy: three-dimensional visualization of neuronal networks in the whole mouse brain. *Nat Methods* 4(4): 331-6.

- Doerr J, Schwarz MK, Wiedermann D, Leinhaas A, Jakobs A, Schloen F, Schwarz I, Diedenhofen M, Braun NC, Koch P, Peterson DA, Kubitscheck U, Hoehn M, Brustle O. 2017. Whole-brain 3D mapping of human neural transplant innervation. *Nat Commun* 8: 14162.
- Fahrbach FO, Gurchenkov V, Alessandri K, Nassoy P, Rohrbach A. 2013a. Light-sheet microscopy in thick media using scanned Bessel beams and two-photon fluorescence excitation. *Opt Express* 21(11): 13824-39.
- Fahrbach FO, Gurchenkov V, Alessandri K, Nassoy P, Rohrbach A. 2013b. Self-reconstructing sectioned Bessel beams offer submicron optical sectioning for large fields of view in light-sheet microscopy. *Opt Express* 21(9): 11425-40.
- Fahrbach FO, Rohrbach A. 2010. A line scanned light-sheet microscope with phase shaped self-reconstructing beams. *Opt Express* 18(23): 24229-44.
- Fahrbach FO, Rohrbach A. 2012. Propagation stability of self-reconstructing Bessel beams enables contrast-enhanced imaging in thick media. *Nat Commun* 3: 632.
- Fehrenbach J, Weiss P, Lorenzo C. 2012. Variational algorithms to remove stationary noise: applications to microscopy imaging. *IEEE Trans Image Process* 21(10): 4420-30.
- Fei P, Lee J, Packard RR, Sereti KI, Xu H, Ma J, Ding Y, Kang H, Chen H, Sung K, Kulkarni R, Ardehali R, Kuo CC, Xu X, Ho CM, Hsiai TK. 2016. Cardiac Light-Sheet Fluorescent Microscopy for Multi-Scale and Rapid Imaging of Architecture and Function. *Sci Rep* 6: 22489.
- Friedrich M, Gan Q, Ermolayev V, Harms GS. 2011. STED-SPIM: Stimulated emission depletion improves sheet illumination microscopy resolution. *Biophys J* 100(8): L43-5.
- Fu Q, Martin BL, Matus DQ, Gao L. 2016. Imaging multicellular specimens with real-time optimized tiling light-sheet selective plane illumination microscopy. *Nature Communications* 7: 11088.
- Gadallah FL, Csillag F, Smith JM. 2000. Destriping multisensor imagery with moment matching. *International Journal of Remote Sensing* 21(12): 2505-2511.
- Galland R, Greci G, Aravind A, Viasnoff V, Studer V, Sibarita JB. 2015. 3D high- and super-resolution imaging using single-objective SPIM. *Nat Methods* 12(7): 641-4.
- Gao L. 2015. Extend the field of view of selective plan illumination microscopy by tiling the excitation light sheet. *Opt Express* 23(5): 6102-11.
- Gao L, Shao L, Chen BC, Betzig E. 2014. 3D live fluorescence imaging of cellular dynamics using Bessel beam plane illumination microscopy. *Nat Protoc* 9(5): 1083-101.
- Gebhardt JC, Suter DM, Roy R, Zhao ZW, Chapman AR, Basu S, Maniatis T, Xie XS. 2013. Single-molecule imaging of transcription factor binding to DNA in live mammalian cells. *Nature Methods* 10(5): 421-6.
- Gohn-Kreuz C, Rohrbach A. 2016. Light-sheet generation in inhomogeneous media using self-reconstructing beams and the STED-principle. *Opt Express* 24(6): 5855-65.
- Greiss F, Deligiannaki M, Jung C, Gaul U, Braun D. 2016. Single-Molecule Imaging in Living Drosophila Embryos with Reflected Light-Sheet Microscopy. *Biophys J* 110(4): 939-46.
- Gualda EJ, Pereira H, Vale T, Estrada MF, Brito C, Moreno N. 2015. SPIM-fluid: open source light-sheet based platform for high-throughput imaging. *Biomed Opt Express* 6(11): 4447-56.
- Gualda EJ, Simao D, Pinto C, Alves PM, Brito C. 2014. Imaging of human differentiated 3D neural aggregates using light sheet fluorescence microscopy. *Front Cell Neurosci* 8: 221.
- Guan Z, Lee J, Jiang H, Dong S, Jen N, Hsiai T, Ho CM, Fei P. 2016. Compact plane illumination plugin device to enable light sheet fluorescence imaging of multi-cellular organisms on an inverted wide-field microscope. *Biomed Opt Express* 7(1): 194-208.
- Guetiérrez-Heredia L, Flood PM, Reynaud EG. 2012. Light Sheet Fluorescence Microscopy: beyond the flatlands In: *Current Microscopy Contributions to Advances*

in Science and Technology. A. Méndez-Vilas E, editor: Formatex Research Center. pp 838-847.

- Hoyer P, de Medeiros G, Balazs B, Norlin N, Besir C, Hanne J, Krausslich HG, Engelhardt J, Sahl SJ, Hell SW, Hufnagel L. 2016. Breaking the diffraction limit of light-sheet fluorescence microscopy by RESOLFT. *Proc Natl Acad Sci U S A* 113(13): 3442-6.
- Hu YS, Zimmerley M, Li Y, Watters R, Cang H. 2014. Single-molecule super-resolution light-sheet microscopy. *Chemphyschem* 15(4): 577-86.
- Huisken J, Stainier DY. 2007. Even fluorescence excitation by multidirectional selective plane illumination microscopy (mSPIM). *Opt Lett* 32(17): 2608-10.
- Huisken J, Stainier DY. 2009. Selective plane illumination microscopy techniques in developmental biology. *Development* 136(12): 1963-75.
- Huisken J, Swoger J, Del Bene F, Wittbrodt J, Stelzer EH. 2004. Optical sectioning deep inside live embryos by selective plane illumination microscopy. *Science* 305(5686): 1007-9.
- Jahr W, Schmid B, Schmied C, Fahrbach FO, Huisken J. 2015. Hyperspectral light sheet microscopy. *Nat Commun* 6: 7990.
- Jeandupeux E, Lobjois V, Ducommun B. 2015. 3D print customized sample holders for live light sheet microscopy. *Biochem Biophys Res Commun* 463(4): 1141-3.
- Ji N, Magee JC, Betzig E. 2008. High-speed, low-photodamage nonlinear imaging using passive pulse splitters. *Nat Meth* 5(2): 197-202.
- Kaufmann A, Mickoleit M, Weber M, Huisken J. 2012. Multilayer mounting enables long-term imaging of zebrafish development in a light sheet microscope. *Development* 139(17): 3242-3247.
- Keller PJ, Ahrens MB. 2015. Visualizing whole-brain activity and development at the single-cell level using light-sheet microscopy. *Neuron* 85(3): 462-83.
- Keller PJ, Ahrens MB, Freeman J. 2015. Light-sheet imaging for systems neuroscience. *Nat Methods* 12(1): 27-9.
- Keller PJ, Schmidt AD, Santella A, Khairy K, Bao Z, Wittbrodt J, Stelzer EHK. 2010. Fast, high-contrast imaging of animal development with scanned light sheet-based structured-illumination microscopy. *Nat Meth* 7(8): 637-642.
- Keller PJ, Schmidt AD, Wittbrodt J, Stelzer EHK. 2008. Reconstruction of Zebrafish Early Embryonic Development by Scanned Light Sheet Microscopy. *Science* 322(5904): 1065-1069.
- Krieger JW, Singh AP, Bag N, Garbe CS, Saunders TE, Langowski J, Wohland T. 2015. Imaging fluorescence (cross-) correlation spectroscopy in live cells and organisms. *Nat Protoc* 10(12): 1948-74.
- Krieger JW, Singh AP, Garbe CS, Wohland T, Langowski J. 2014. Dual-color fluorescence cross-correlation spectroscopy on a single plane illumination microscope (SPIM-FCCS). *Opt Express* 22(3): 2358-75.
- Krzic U, Gunther S, Saunders TE, Streichan SJ, Hufnagel L. 2012. Multiview light-sheet microscope for rapid in toto imaging. *Nat Methods* 9(7): 730-3.
- Lavagnino Z, Dwight J, Ustione A, Nguyen TU, Tkaczyk TS, Piston DW. 2016a. Snapshot Hyperspectral Light-Sheet Imaging of Signal Transduction in Live Pancreatic Islets. *Biophys J* 111(2): 409-17.
- Lavagnino Z, Sancataldo G, d'Amora M, Follert P, De Pietri Tonelli D, Diaspro A, Cella Zanacchi F. 2016b. 4D (x-y-z-t) imaging of thick biological samples by means of Two-Photon inverted Selective Plane Illumination Microscopy (2PE-iSPIM). *Sci Rep* 6: 23923.
- Lemon WC, Keller PJ. 2015. Live imaging of nervous system development and function using light-sheet microscopy. *Mol Reprod Dev* 82(7-8): 605-18.
- Liang X, Zang Y, Dong D, Zhang L, Fang M, Yang X, Arranz A, Ripoll J, Hui H, Tian J. 2016. Stripe artifact elimination based on nonsubsampling contourlet transform for light sheet fluorescence microscopy. *J Biomed Opt* 21(10): 106005.
- Mahou P, Vermot J, Beaurepaire E, Supatto W. 2014. Multicolor two-photon light-sheet microscopy. *Nat Methods* 11(6): 600-1.

- Mayer J, Robert-Moreno A, Danuser R, Stein JV, Sharpe J, Swoger J. 2014. OPTiSPIM: integrating optical projection tomography in light sheet microscopy extends specimen characterization to nonfluorescent contrasts. *Opt Lett* 39(4): 1053-6.
- Meddens MB, Liu S, Finnegan PS, Edwards TL, James CD, Lidke KA. 2016. Single objective light-sheet microscopy for high-speed whole-cell 3D super-resolution. *Biomed Opt Express* 7(6): 2219-36.
- Münch B, Trtik P, Marone F, Stampanoni M. 2009. Stripe and ring artifact removal with combined wavelet — Fourier filtering. *Optics Express* 17(10): 8567-8591.
- Novak D, Kucharova A, Ovecka M, Komis G, Samaj J. 2015. Developmental Nuclear Localization and Quantification of GFP-Tagged EB1c in Arabidopsis Root Using Light-Sheet Microscopy. *Front Plant Sci* 6: 1187.
- Olarte OE, Andilla J, Artigas D, Loza-Alvarez P. 2015. Decoupled illumination detection in light sheet microscopy for fast volumetric imaging. *Optica* 2(8): 702-705.
- Olarte OE, Licea-Rodriguez J, Palero JA, Gualda EJ, Artigas D, Mayer J, Swoger J, Sharpe J, Rocha-Mendoza I, Rangel-Rojo R, Loza-Alvarez P. 2012. Image formation by linear and nonlinear digital scanned light-sheet fluorescence microscopy with Gaussian and Bessel beam profiles. *Biomed Opt Express* 3(7): 1492-505.
- Ovecka M, Vaskebova L, Komis G, Luptovciak I, Smertenko A, Samaj J. 2015. Preparation of plants for developmental and cellular imaging by light-sheet microscopy. *Nat Protoc* 10(8): 1234-47.
- Paie P, Bragheri F, Bassi A, Osellame R. 2016. Selective plane illumination microscopy on a chip. *Lab Chip* 16(9): 1556-60.
- Palayret M, Armes H, Basu S, Watson AT, Herbert A, Lando D, Etheridge TJ, Endesfelder U, Heilemann M, Laue E, Carr AM, Klenerman D, Lee SF. 2015. Virtual-'light-sheet' single-molecule localisation microscopy enables quantitative optical sectioning for super-resolution imaging. *PLoS One* 10(4): e0125438.
- Pampaloni F, Chang BJ, Stelzer EH. 2015. Light sheet-based fluorescence microscopy (LSFM) for the quantitative imaging of cells and tissues. *Cell Tissue Res* 360(1): 129-41.
- Planchon TA, Gao L, Milkie DE, Davidson MW, Galbraith JA, Galbraith CG, Betzig E. 2011. Rapid three-dimensional isotropic imaging of living cells using Bessel beam plane illumination. *Nat Methods* 8(5): 417-23.
- Ploschner M, Kollarova V, Dostal Z, Nyk J, Barton-Owen T, Ferrier DE, Chmelik R, Dholakia K, Cizmar T. 2015. Multimode fibre: Light-sheet microscopy at the tip of a needle. *Sci Rep* 5: 18050.
- Regmi R, Mohan K, Mondal PP. 2013. Light sheet based imaging flow cytometry on a microfluidic platform. *Microscopy Research and Technique* 76(11): 1101-1107.
- Reynaud EG, Peychl J, Huysken J, Tomancak P. 2015. Guide to light-sheet microscopy for adventurous biologists. *Nat Methods* 12(1): 30-4.
- Rocha-Mendoza I, Licea-Rodriguez J, Marro M, Olarte OE, Plata-Sanchez M, Loza-Alvarez P. 2015. Rapid spontaneous Raman light sheet microscopy using cw-lasers and tunable filters. *Biomed Opt Express* 6(9): 3449-61.
- Scheul T, Wang I, Vial JC. 2014. STED-SPIM made simple. *Opt Express* 22(25): 30852-64.
- Silvestri L, Bria A, Sacconi L, Iannello G, Pavone FS. 2012. Confocal light sheet microscopy: micron-scale neuroanatomy of the entire mouse brain. *Opt Express* 20(18): 20582-98.
- Smyrek I, Stelzer EH. 2017. Quantitative three-dimensional evaluation of immunofluorescence staining for large whole mount spheroids with light sheet microscopy. *Biomed Opt Express* 8(2): 484-499.
- Swoger J, Verveer P, Greger K, Huysken J, Stelzer EH. 2007. Multi-view image fusion improves resolution in three-dimensional microscopy. *Opt Express* 15(13): 8029-42.
- Taormina MJ, Jemielita M, Stephens WZ, Burns AR, Troll JV, Parthasarathy R, Guillemin K. 2012. Investigating bacterial-animal symbioses with light sheet microscopy. *Biol Bull* 223(1): 7-20.

- Tomer R, Khairy K, Amat F, Keller PJ. 2012. Quantitative high-speed imaging of entire developing embryos with simultaneous multiview light-sheet microscopy. *Nat Methods* 9(7): 755-63.
- Tomer R, Lovett-Barron M, Kauvar I, Andalman A, Burns VM, Sankaran S, Grosenick L, Broxton M, Yang S, Deisseroth K. 2015. SPED Light Sheet Microscopy: Fast Mapping of Biological System Structure and Function. *Cell* 163(7): 1796-806.
- Trivedi V, Truong TV, Trinh le A, Holland DB, Liebling M, Fraser SE. 2015. Dynamic structure and protein expression of the live embryonic heart captured by 2-photon light sheet microscopy and retrospective registration. *Biomed Opt Express* 6(6): 2056-66.
- Truong TV, Supatto W, Koos DS, Choi JM, Fraser SE. 2011. Deep and fast live imaging with two-photon scanned light-sheet microscopy. *Nat Meth* 8(9): 757-760.
- Udan RS, Piazza VG, Hsu CW, Hadjantonakis AK, Dickinson ME. 2014. Quantitative imaging of cell dynamics in mouse embryos using light-sheet microscopy. *Development* 141(22): 4406-14.
- Vettenburg T, Dalgarno HI, Nylk J, Coll-Llado C, Ferrier DE, Cizmar T, Gunn-Moore FJ, Dholakia K. 2014. Light-sheet microscopy using an Airy beam. *Nat Methods* 11(5): 541-4.
- Voie AH, Burns DH, Spelman FA. 1993. Orthogonal-plane fluorescence optical sectioning: three-dimensional imaging of macroscopic biological specimens. *J Microsc* 170(Pt 3): 229-36.
- Weber M, Huiskens J. 2012. Omnidirectional microscopy. *Nat Meth* 9(7): 656-657.
- Weber M, Huiskens J. 2015. In vivo imaging of cardiac development and function in zebrafish using light sheet microscopy. *Swiss Med Wkly* 145: w14227.
- Weber M, Mickoleit M, Huiskens J. 2014. Multilayer mounting for long-term light sheet microscopy of zebrafish. *J Vis Exp*(84): e51119.
- Wolf S, Supatto W, Debregeas G, Mahou P, Kruglik SG, Sintès JM, Beaurepaire E, Candelier R. 2015. Whole-brain functional imaging with two-photon light-sheet microscopy. *Nat Methods* 12(5): 379-80.
- Wu Y, Wawrzusin P, Senseney J, Fischer RS, Christensen R, Santella A, York AG, Winter PW, Waterman CM, Bao Z, Colon-Ramos DA, McAuliffe M, Shroff H. 2013. Spatially isotropic four-dimensional imaging with dual-view plane illumination microscopy. *Nat Biotechnol* 31(11): 1032-8.
- Yang Z, Prokopas M, Nylk J, Coll-Llado C, Gunn-Moore FJ, Ferrier DE, Vettenburg T, Dholakia K. 2014. A compact Airy beam light sheet microscope with a tilted cylindrical lens. *Biomed Opt Express* 5(10): 3434-42.
- Zagato E, Brans T, Verstuyft S, van Thourhout D, Missinne J, van Steenberge G, Demeester J, De Smedt S, Remaut K, Neyts K, Braeckmans K. 2017. Microfabricated devices for single objective single plane illumination microscopy (SoSPIM). *Optics Express* 25(3): 1732-1745.
- Zhang P, Phipps ME, Goodwin PM, Werner JH. 2016. Light-sheet microscopy by confocal line scanning of dual-Bessel beams. *J Biomed Opt* 21(10): 100502.
- Zhao M, Zhang H, Li Y, Ashok A, Liang R, Zhou W, Peng L. 2014. Cellular imaging of deep organ using two-photon Bessel light-sheet nonlinear structured illumination microscopy. *Biomed Opt Express* 5(5): 1296-308.
- Zhao T, Lau SC, Wang Y, Su Y, Wang H, Cheng A, Herrup K, Ip NY, Du S, Loy MM. 2016. Multicolor 4D Fluorescence Microscopy using Ultrathin Bessel Light Sheets. *Sci Rep* 6: 26159.
- Zong W, Chen X, Zhao J, Zhang Y, Fan M, Zhou Z, Cheng H, Sun Y, Chen L. Two-photon three-axis digital scanned light-sheet microscopy (2P3A-DSLM). *OSA Technical Digest* (online); 2014 2014/06/08; San Jose, California. Optical Society of America. p AW3L.7.
- Zong W, Zhao J, Chen X, Lin Y, Ren H, Zhang Y, Fan M, Zhou Z, Cheng H, Sun Y, Chen L. 2015. Large-field high-resolution two-photon digital scanned light-sheet microscopy. *Cell Res* 25(2): 254-7.

TABLES

Table 1					
Type beam	λ_{ill}	$NA_{ill\ lens}$	LS thickness	FoV	Reference
Gaussian (cyl)	488 nm 543 nm 633 nm	0.16	2-4 μm	N.A.	Pampaloni et al. (2015)
Gaussian (DLISM)	488 nm 532 nm	0.42	$\sim 2\ \mu m$	16 μm	Vettenburg et al. (2014)
Bessel	488 nm 532 nm	0.42	$\sim 2\ \mu m$	42 μm	Vettenburg et al. (2014)
Ultrathin Bessel	488 nm 560 nm	0.7	0.6 μm	15 μm	Zhao et al. (2016)
Lattice	560 nm	0.55	N.A.	100 μm	(Chen et al.)
Airy	488 nm 532 nm	0.42	$\sim 0.9\ \mu m$	346 μm	Vettenburg et al. (2014)
2PE Bessel	Near-Infrared	0.5	0.5 μm	60-80 μm	Planchon et al. (2011)
(Tiling) Bessel	488 nm 560 nm	0.8	$\sim 1.2\ \mu m$	200 μm	Fu et al. (2016)
2PE 3A-DLSM	680 nm 1080 nm	0.3	$\sim 3\ \mu m$	Variable (till 500 μm)	Zong et al. (2014)

Table 1: Summary of the characteristics of the light sheets discussed in section "Engineered light sheets" N.A. = not available

FIGURES

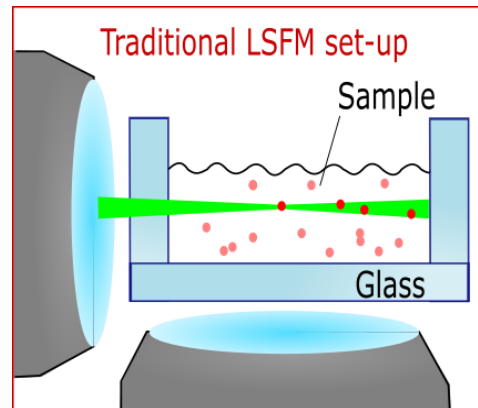


Figure 1: Traditional configuration of objective lenses and the sample in a light sheet microscope. A thin plane in the sample is illuminated by an objective lens placed orthogonally with respect to the objective lens used for detection. Such a configuration reduces the background noise and total light exposure of the sample by only illuminating the focal plane of the imaging lens.

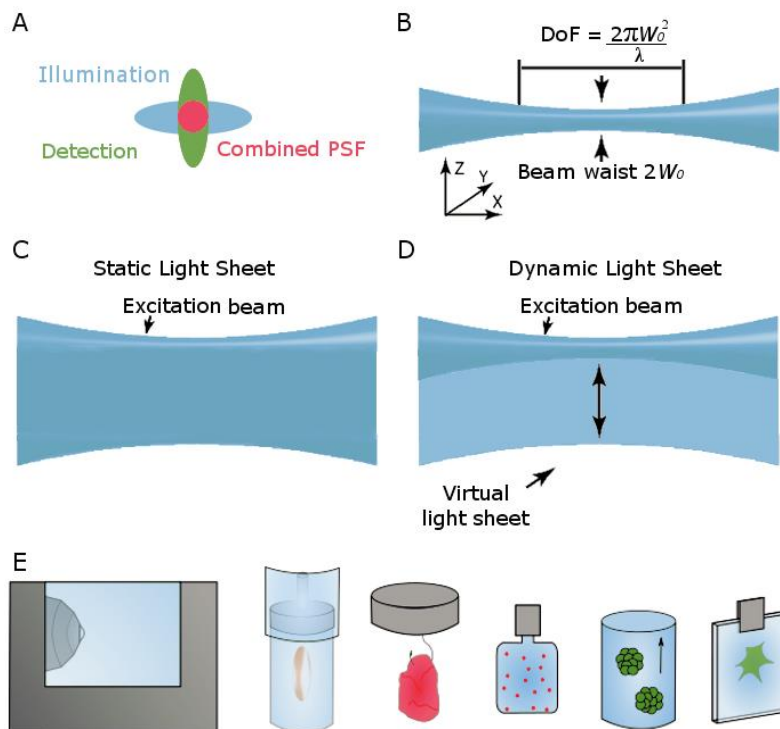


Figure 2. (A) The PSF of an LSFM system is the product of the PSF of the illumination and the detection objective lens. (B) A Gaussian beam is defined by its beam waist W_0 and its depth of field DoF. (C) and (D) illustrate a static and dynamic light sheet, respectively. (E) Example of a water-filled chamber (only one of two objective lenses is shown) and

its sample holders that are dipped into the water bath. The samples are, respectively, embedded in agarose gel, hooked to the holder, enclosed in a transparent bag, flowing through a channel or adherently attached to a coverslip.

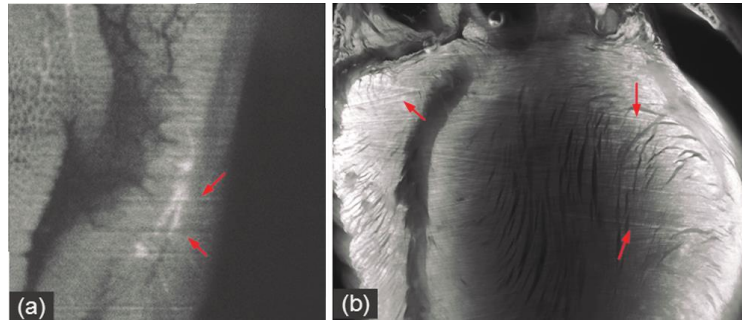


Figure 3. Stripes are a common artefact in LSFM images: (a) a slice of mouse colon imaged with a custom-made unidirectional LSFM system and (b) a slice of mouse heart imaged with a multidirectional LSFM system. The red arrows indicate some prominent stripes. Adapted with permission from Liang et al. (2016).

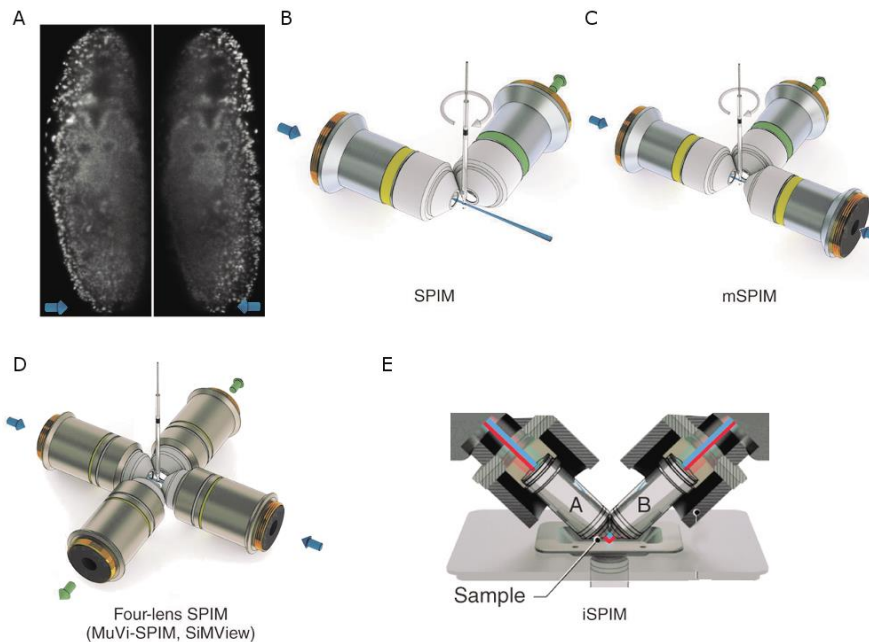


Figure 4. (A) An image of a *Drosophila* embryo illuminated from the left and from the right. The degradation of the image quality along the illumination direction is evident. Adapted with permission from de Medeiros et al. (2015), licensed under Creative Commons CC-BY 4.0 license (B) A basic SPIM set-up. The sample is rotated to collect multiview images of the specimen, that will be later reconstructed into a 3D figure. (C) In mSPIM two objective lenses provide illumination to the specimen from opposing sides to enhance illumination uniformity. (D) MuVi-SPIM and SiMView systems consist of two lenses used for illumination and two lenses used for detection. (E) Dual inverted SPIM. To achieve isotropic resolution, both lenses are identical and are used alternatively to illuminate and image the sample. Image B,C,D are reprinted by permission from Macmillan Publishers Ltd: NATURE METHODS, from Weber and Huisken (2012), copyright 2012. Image E is reprinted with permission from Springer Nature, Nature Biotechnology, from Wu et al. 2013, Copyright 2013.

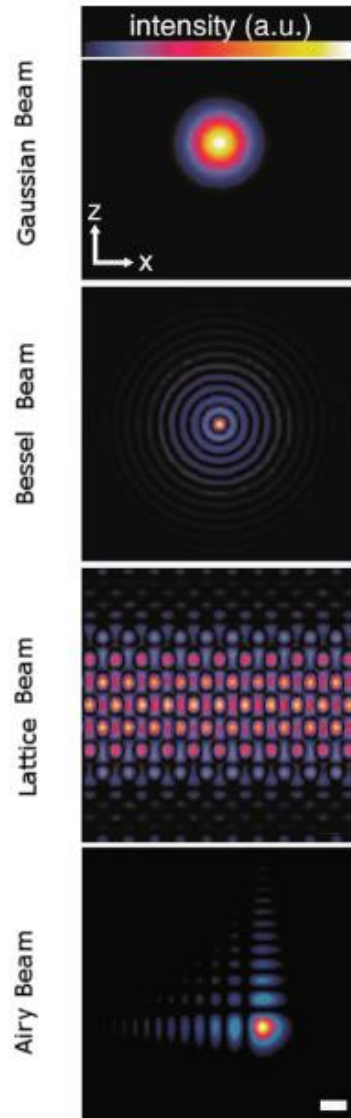


Figure 5. Different beam shapes that have been used to create dynamic light sheets for LSFM. Modified from Chen et al. (2014). Reprinted with permission from AAAS.

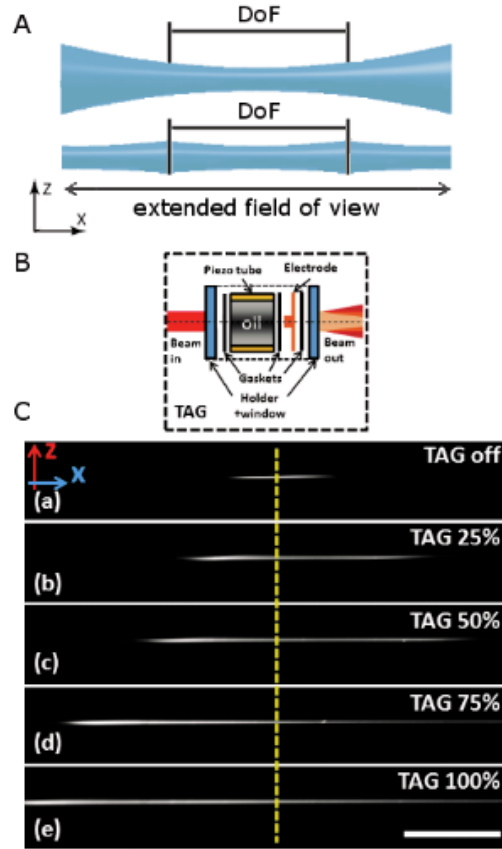


Figure 6. (A) Working principle of tiling. A tiled light sheet can be obtained by considering only the signal that comes from the thinner region of the Gaussian beam. By moving its focus an image with extended field of view is obtained. (B) Scheme of a tunable acoustic gradient index device (TAG), used to scan the focal spot along the illumination axis of the beam. (C) Using the TAG index device, the DoF of the light sheet (a)-(e) can be tailored between $50\ \mu\text{m}$ to $500\ \mu\text{m}$ with constant FWHM of $3\ \mu\text{m}$. Scale bar: $100\ \mu\text{m}$. Adapted with permission from Zong et al. (2014).

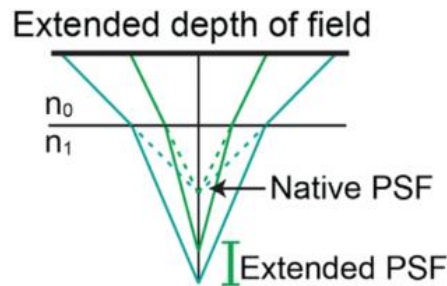


Figure 7. A simple method to extend the depth of field of the detection lens makes use of spherical aberrations cleverly introduced by stratified refractive indexes in front of the detection lens. Reprinted and adapted from Tomer et al. (2015), Copyright 2015, with permission from Elsevier.

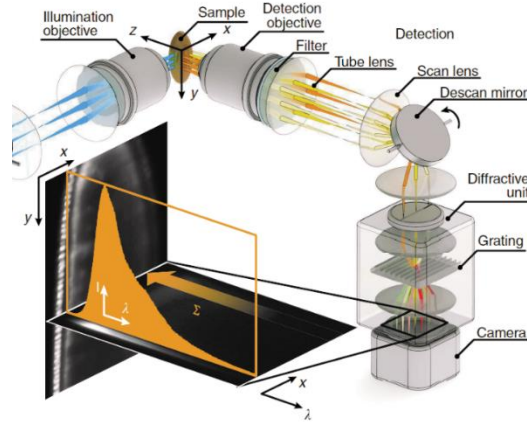


Figure 8. Schematic representation of an hyperspectral LSFM set-up. The light sheet is created by quickly scanning the illumination beam (Jahr et al., 2015) with a scanning mirror. The sample is placed at the intersection of the focal planes of the detection and illumination objective lenses and illuminated with the scanned light sheet. The fluorescence signal is descanned onto a single line with a second scan mirror. A diffractive unit separates the spectral components of the incoming light spatially. On the camera chip, a stack of x, λ -data sets is recorded, resulting in a three-dimensional data cube. Summing over all wavelengths would yield the conventional, single-colour image. Obtained by Jahr et al. (2015) licensed under Creative Commons CC-BY 4.0 license.

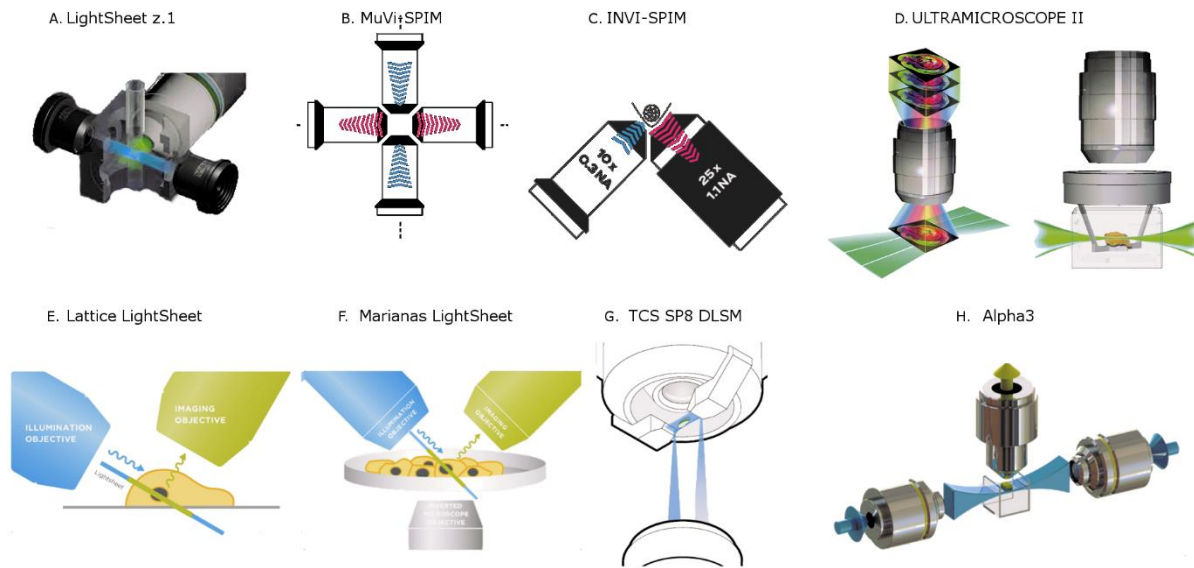


Figure 9. Several commercially available LSFM configurations. A) A detailed view of the sample chamber of the LightSheet z.1 microscope (Zeiss). The sample is placed in the chamber from above and it is illuminated from two opposing sides with light sheet illumination. Source: <https://www.zeiss.com/microscopy/us/products/imaging-systems/lightsheet-z-1.html> B) Top view of the configuration of objective lenses in a MuVi-SPIM microscope (Luxendo). Illumination is indicated with blue lines, detection with purple lines. Source: <http://luxendo.eu/> C) Side view of the configuration of objective lenses in an InVi-SPIM (Luxendo). Source: <http://luxendo.eu/invi-spim> D) Schematic representation of an Ultramicroscope II (LaVisionBioTech). The sample is illuminated from two sides by 6 light sheets whose focus can be rapidly shifted through the sample. Source: <http://www.lavisionbiotech.com/ultramicroscope-ii-technology.html> E) Side view of the objective lenses in the Lattice Lightsheet microscope (3i). The sample is mounted on a round coverslip, placed in water and illuminated by a $0.4 \mu\text{m}$ thin lattice light sheet. Source: <https://www.intelligent-imaging.com/> F) Marianas Lightsheet (3i) places a dual inverted SPIM set-up on an inverted live-cell microscope system to allow the combination of multiple imaging modalities. Source: <https://www.intelligent-imaging.com/> G) Close view of the TwinFlect mirror device used in the TCS SP8 Digital Light Sheet microscope (Leica). The laser light is reflected horizontally by two opposing mirrors and imaging is performed through the microscope's objective lens. This configuration allows the implementation of other imaging modalities and techniques. Source: <http://www.leica-microsystems.com/products/confocal->

[microscopes/details/product/leica-tcs-sp8-dls/H](https://www.leica-microscopes/details/product/leica-tcs-sp8-dls/H)) The Alpha³ microscope (Phaseview) is composed of modular parts that can be separately added to existing microscopes. Source: <http://www.alphalightsheet.com/>

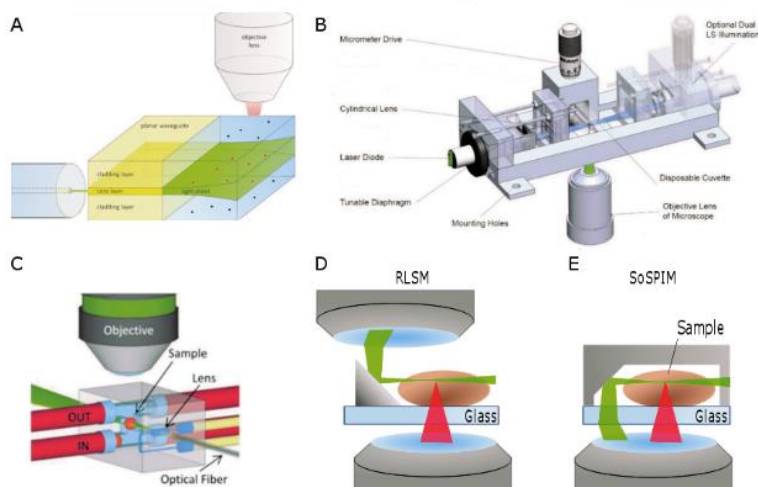


Figure 10. Strategies that integrate LSFM on traditional epi-fluorescence microscopes. (A) Schematic representation of Deschout's sample holder. Through butt-coupling of a single mode fiber, the laser light travels through a planar waveguide and forms a light sheet in the channel. Fluorescent light is collected by an objective lens positioned above or below the sample holder. Adapted from Deschout et al. (2014) with permission from The Royal Society of Chemistry. (B) Scheme of PIP device (Guan et al., 2016). The device is mounted directly on the microscope body and is already equipped with a compact laser and cylindrical lens. The sample is placed in a disposable cuvette and imaged through the objective lens of the microscope. (C) Optofluidic device for high throughput analysis of spheroids. An embedded, liquid-filled cylindrical lens focuses the laser light coming from an optical fiber into a microfluidic channel. The sample flows at a constant speed through the light sheet, allowing quick scanning of the specimens. Reproduced with permission from Paie et al. (2016), licensed under Creative Commons CC-BY 3.0 license (D) A typical Reflected Light Sheet Microscope (RLSM). The laser beam, coming from a modified condenser, is reflected horizontally on the sample by a 45° mirror. The emitted photons are collected by the objective lens of the microscope. (E) A single-lens variant of RLSM, called SoSPIM. The excitation light is provided through the same objective lens used for detection. The light is reflected horizontally into the sample holder by a microfabricated micromirror.

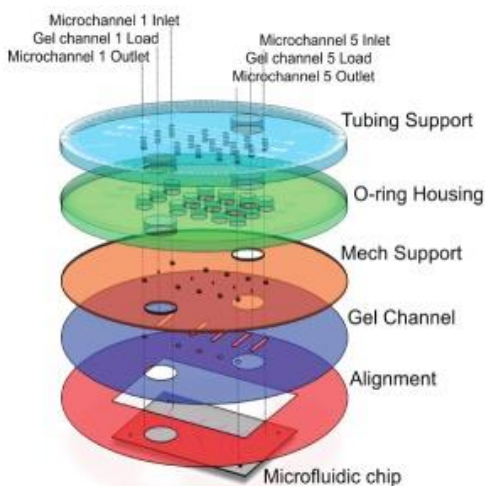


Figure 11. Exploded view of Meddens' chip packaging.